

Temperature excursions during the transient behaviour of high temperature catalytic combustion monoliths

Almerinda Di Benedetto*, Stefano Cimino, Raffaele Pirone, Gennaro Russo

Istituto Ricerche sulla Combustione—CNR, P. le Tecchio 80, 80125 Naples, Italy

Received 1 May 2002; received in revised form 28 November 2002; accepted 18 March 2003

Abstract

Spatio-temporal temperature profiles experimentally observed during the operation of a structured perovskite-based catalytic monolith for the combustion of methane were simulated by means of a transient heterogeneous one-dimensional model which accounts for heat losses to the surroundings and thermal conductivity inside the monolith substrate. In fact it is shown that such thermal phenomena are essential to correctly reproduce the slow warm-up transients and the wrong-way behaviour observed in a low conductivity ceramic monolith. Model simulations reveal that at higher values of solid conductivity the catalyst does not exhibit hot spot both in time and space, but needs higher inlet gas temperatures to reach complete methane conversion. Bifurcation analysis of the catalytic monolith reactor model were carried out to study steady-state multiplicity. We show that the origin of multiplicity is purely thermal as it is mainly ruled by the heat transfer through the external surface.

© 2003 Elsevier B.V. All rights reserved.

Keywords: Transient; Catalytic combustion; Monolith; Wrong-way behaviour; Steady-state multiplicity; Modelling

1. Introduction

Catalytic combustion in structured reactors is an effective clean technology for both adiabatic and radiant burners in industrial and domestic applications. In recent years a considerable amount of research has been devoted to the study of catalysts (mainly noble metals), reactor configurations and optimal steady-state operating conditions for such processes [1–14].

During their lifetime, catalytic combustors are subjected to transient operations due to changes in conditions and start-up/shut-down. During all these operations complex temperature patterns may arise leading to hot spot formation and wrong-way behaviour which

must be controlled to preserve the catalyst durability [2,4,8,9,14].

Several mathematical models of catalytic combustors have been developed to describe steady operations as well as evolution of gas composition and temperatures during the transient phases [2,4–8,14,15], mainly under the assumption of fully adiabatic systems. It has been shown that catalytic combustors may exhibit steady-state multiplicity [4,10,17] and that wrong-way behaviour may arise as the reactor response to step change of gas inlet temperature [2].

Experimental results of catalytic combustion in monolithic reactors show that steady and transient behaviour can be both qualitatively and quantitatively different from that of adiabatic ones [11,12,18,19] suggesting that heat losses can play a relevant role in monolith combustor performance.

* Corresponding author.

E-mail address: dibenede@irc.na.cnr.it (A. Di Benedetto).

Nomenclature

| | |
|-------------------------------|--|
| a_v | gas–solid surface per unit gas volume (m^2/m^3) |
| $a_{v,s}$ | gas–solid surface per unit solid volume (m^2/m^3) |
| C_g | total gas concentration (mol/m^3) |
| C_{pg} , C_{ps} | gas and solid heat capacity, respectively ($\text{J}/(\text{kg K})$) |
| d | diameter of monolith channel (m) |
| E_{act} | activation energy (J/mol) |
| h_g | gas–solid heat transfer coefficient ($\text{W}/\text{m}^2 \text{K}$) |
| ΔH | heat of reaction (J/mol) |
| k_g | gas–solid mass transfer coefficient (m/s) |
| k^0 | kinetic constant ($\text{m}^3/\text{kg}_{\text{cat}} \text{s}$) |
| L | reactor length (m) |
| Nu | Nusselt number |
| R | gas constant ($\text{J}/\text{mol K}$) |
| R_{CH_4} | catalytic reaction rate (s^{-1}) |
| Sh | Sherwood number |
| t | time (s) |
| T_F | oven temperature (K) |
| T_g | gas temperature (K) |
| T_{preheat} | gas preheat temperature (K) |
| T_s | solid temperature (K) |
| T_s^0 | initial catalyst temperature (K) |
| U | global radial exchange coefficient per solid volume ($\text{W}/\text{m}^3 \text{K}$) |
| v_g | superficial gas velocity (m/s) |
| x_{CH_4} | methane molar fraction in the gas phase |
| $x_{\text{CH}_4}^{\text{in}}$ | methane inlet molar fraction in gas |
| $x_{\text{CH}_4}^s$ | methane molar fraction on catalyst |
| z | axial position (m) |

Greek letters

| | |
|--------------------------|---|
| α | solid thermal diffusivity (m^2/s) |
| α_s | total surface area over solid surface |
| δ | thermocouple lag |
| ε | catalyst emissivity |
| λ_s | solid thermal conductivity ($\text{W}/\text{m K}$) |
| $\lambda_{s,\text{rad}}$ | equivalent thermal conductivity for radiation ($\text{W}/\text{m K}$) |
| ρ_g | gas density (kg/m^3) |
| ρ_s | apparent catalyst density (kg/m^3) |
| σ | Stephan–Boltzmann constant ($\text{W}/\text{m}^2 \text{K}^4$) |

In a previous paper, we showed the results of a relatively simple mathematical model which is able to satisfactorily reproduce the ignition experimentally observed over a perovskite-based monolithic catalyst, tested in the lean premixed combustion of methane under non-adiabatic conditions [11].

The experimental results obtained on that reactor showed the appearance and the travelling of strong hot spots during transient operations or changing flow rate and preheat temperature. We also observed the existence of a hysteresis as a function of the gas inlet temperature [11].

In this work, the temperature excursions arising on the catalyst were investigated by means of a mathematical model to examine the effect of thermal phenomena and of changes in operating conditions on the transient behaviour of the monolith. We also discuss the ignition/extinction behaviour of the monolith in the parameter space related to thermal phenomena, such as the heat transfer coefficient, thermal conductivity and inlet gas temperature by means of bifurcation analysis.

2. Mathematical model development

The catalytic monolith reactor is as an array of 24 uniform and open channels arranged in the form of a honeycomb characterised by 5×5 geometry with the central channel blocked to gas flow to host three thermocouples [12]. In this configuration, only two channels are present in the radial direction with a characteristic length of 2.6 mm. Due to the presence of external heat losses, radial gradients inside the monolith can be expected if the solid connected matrix does not help to equalise the temperature profiles. Evaluation of the effective radial thermal conductivity according the Groppi and Tronconi formula [26] allows the comparison of the external and internal resistance to heat transfer: it results that the temperature variation across the monolith in the radial direction is always limited to less than 4% of the external difference between the catalyst wall and the environment. Therefore the strong simplification obtained by assuming radial isothermicity is justified. This simplification allows us to perform the bifurcation analysis. Radial variations of temperature and concentrations in the gas phase have been integrated resulting in lumped

values which are assumed to vary along the axial distance. Heat and mass transfer coefficients have been used to model fluxes between the solid and the bulk gas phases. As pointed out by Gupta et al. [20], only with proper Nu and Sh correlations, can excellent approximations be obtained using one-dimensional models if the Pe number is much lower than 1. It is worth noting that at the moment no commonly accepted correlations are available for the evaluation of heat and mass transfer coefficients in catalytic monoliths. The correlations experimentally derived by Ullah et al. [22] and Votruba et al. [23] in reacting conditions and concerning the light-off point, suffer from significant errors since obtained in the presence of a non-completely mass transfer controlled regime, as pointed out by Hayes and Kolaczkowski [24].

In the present paper, correlations proposed by Hawthorn [21] evaluated at the mean of inlet and outlet conditions, are used to calculate Nu and Sh numbers. This choice is justified by the lower activity of perovskites if compared to Pd-based catalysts, which prevents a sharp transition from kinetically to mass transfer limited regimes at light-off, usually associated with the largest discrepancy of Nu and Sh numbers from their asymptotic values [20,25].

In the monolith under study heat losses are assumed to occur both in the radial and axial directions, respectively, by conduction through the outer shell and by radiation from inlet and outlet surfaces of the monolith. The overall radial heat transfer coefficient, U , has been calculated as the inverse of the sum of resistance in series while the emissivity has been estimated by means of a global heat balance on the reactor.

All other model hypotheses have been elsewhere discussed in more detail [11].

The model equations are the following:

Gas phase mass balance, CH_4 :

$$v_g \left(\frac{\partial x_{CH_4}}{\partial z} \right) = -k_g a_v (x_{CH_4} - x_{CH_4}^s) \quad (1)$$

Boundary condition:

$$\text{At } z = 0, \quad x_{CH_4} = x_{CH_4}^{\text{in}} \quad (1a)$$

Solid phase mass balance, CH_4 :

$$k_g a_{v,s} (x_{CH_4} - x_{CH_4}^s) = R_{CH_4} \quad (2)$$

Gas phase energy balance:

$$v_g \rho_g C_{pg} \left(\frac{\partial T_g}{\partial z} \right) = h_g a_v (T_g - T_s) \quad (3)$$

The Dirichlet boundary conditions are used in the model:

$$\text{At } z = 0, \quad T_g = T_{\text{preheat}} \quad (3a)$$

Solid phase energy balance:

$$\rho_s C_{ps} \left(\frac{\partial T_s}{\partial t} \right) = \lambda_s \left(\frac{\partial^2 T_s}{\partial z^2} \right) + \delta h_g a_{v,s} (T_g - T_s) + \delta \Delta R_{CH_4} C_g + U(T_F - T_s) \quad (4)$$

Initial condition:

$$t = 0, \quad T_s = T_s^0 \quad (4a)$$

T_s^0 is assumed as constant and equal to the gas preheating temperature (T_{preheat}) in all the runs except in the simulations of hysteresis in which the catalyst temperature profile of the previously calculated steady state is used as the initial condition for the solid temperature.

The boundary conditions are:

$$\text{At } z = 0, \quad \lambda_s \frac{\partial T_s}{\partial z} = \alpha_s \sigma \varepsilon (T_s^4 - T_F^4) \quad (4b)$$

$$\text{At } z = L, \quad -\lambda_s \frac{\partial T_s}{\partial z} = \alpha_s \sigma \varepsilon (T_s^4 - T_F^4) \quad (4c)$$

In all the simulations the oven temperature is assumed constant and equal to the gas preheating temperature.

The reaction rate used in the calculations is the following:

$$R_{CH_4} = k^0 \exp \left(\frac{-E_{\text{act}}}{RT} \right) x_{CH_4}^{0.8} \rho_s \quad (5)$$

Kinetic parameters in Eq. (5) have been independently evaluated by means of isothermal measurements of methane oxidation [11,12]. The values of parameters used in most simulations are given in Table 1.

The set of partial differential equations (1)–(4) with boundary ((1a), (3a), (4b) and (4c)) and initial conditions ((4a)) was first reduced to a system of ordinary differential equations by applying a finite difference scheme. The resulting system of ordinary differential equations has been solved by using the Gear algorithm [27] to perform transient simulations. Bifurcation analysis was carried out by solving

Table 1
List of model parameter values

| Parameter | Value |
|-------------------------------|----------|
| v_g (m/s) | 1.5 |
| $x_{CH_4 in}$ | 0.03 |
| C_{ps} (J/kg K) | 600 |
| ρ_s (kg/m ³) | 2260 |
| λ_s (W/m K) | 3 |
| L (m) | 0.46 |
| d (m) | 0.001086 |
| ε | 0.75 |
| h_g (W/m ² K) | 210 |
| U (W/m ³ K) | 20000 |

the obtained system of ordinary differential equations by means of the continuation method using the software AUTO [28]. Since the discretised forms of the boundary conditions in the solid phase energy balance ((4a) and (4b)) are implicit equations of the solid temperature, it was necessary to explicitly calculate the solid temperature as a function of the parameters. An explicit formula easily implemented in the AUTO code was obtained using the symbolic expression given by the software MAPLE [29].

3. Results

In a previous paper we showed that during the start-up, hot spots arise on the catalyst surface of the perovskite-based honeycomb-type monolith [11]. In Fig. 1A both experimental and computed catalyst temperatures are plotted as a function of reactor length at different times during warm-up. As already discussed [11], catalyst temperature initially increases in the sections close to the outlet of the monolith. After about 22 min the catalyst temperature starts to increase more steeply, giving rise to a heat wave travelling backwards towards the inlet sections of the monolith in about 20 min. The steady-state temperature profile which is reached after about 40 min displays a maximum in the region close to the entrance. The maximum is the result of the coupling between the heat losses to the surrounding and the heat produced by reaction. Simulations (Fig. 1B) show that in the early stages of ignition, methane conversion reaches about 80%. After 25 min from the start of the

run, the outlet methane conversion goes to completion (about 100%) while the temperature profile is still developing inside the channel (Fig. 1A). There is a phase shift of about 20 min between the time required to reach a complete fuel conversion and the time to reach a steady-state operating point. During this time the travelling heat front together with the light-off point, e.g. the point of sudden CH₄ concentration change (from inlet value to nil), move backwards.

This behaviour can be explained by observing that in the early stages of warm-up, reaction occurs at sections close to the outlet. The upstream section of the monolith is heated by the axial conduction heat transfer through the support allowing the reaction front to stabilise at the inlet of the channel. Simulations performed neglecting the heat conduction term in Eq. (4) reveal that light-off point is steadily positioned close to the outlet section of the catalyst, while the inlet zone stays relatively cold also after ignition. To model the experimental temperature profiles and the time scales of heat wave travelling (Fig. 1A) we used the support thermal conductivity λ_s as the fitting parameter [11]: the obtained value $\lambda_s = 3$ W/m K is reasonable for a ceramic monolith, as it corresponds to the conductivity of cordierite substrates [9], slightly increased to account for the contribution of heat exchanged by radiation inside the channel in the axial direction [30,31]. According to the findings of Lee and Airs [31], the contribution of internal radiation can be approximated as a conductive flux in which the equivalent thermal conductivity is calculated according to the following formula:

$$\lambda_{s,rad} = \frac{8}{3}\sigma d T_s^3 \Psi(\chi)$$

where $\chi = L/d \cong 42$, and $\Psi(\chi) \rightarrow 1$ for the large value of χ , which at the end gives $\lambda_{s,rad} = 0.26$ W/m K at $T_s = 900$ °C. The radiative heat transfer contribution is then small due to the high aspect ratio.

The time required by the heat wave to travel from the outlet towards the inlet of the channel is of the same order of magnitude of the axial heat diffusion time ($t_c = L^2/\alpha \approx 17$ min, where α is the solid thermal diffusivity, $\alpha = \lambda_s/\rho_s C_{ps}$). This confirms that the heat transferred in the axial direction by conduction and internal radiation is the mechanism responsible for the shift of the light-off position. The long time required to ignite the reaction and reach 100% methane conversion (about 25 min) is determined by

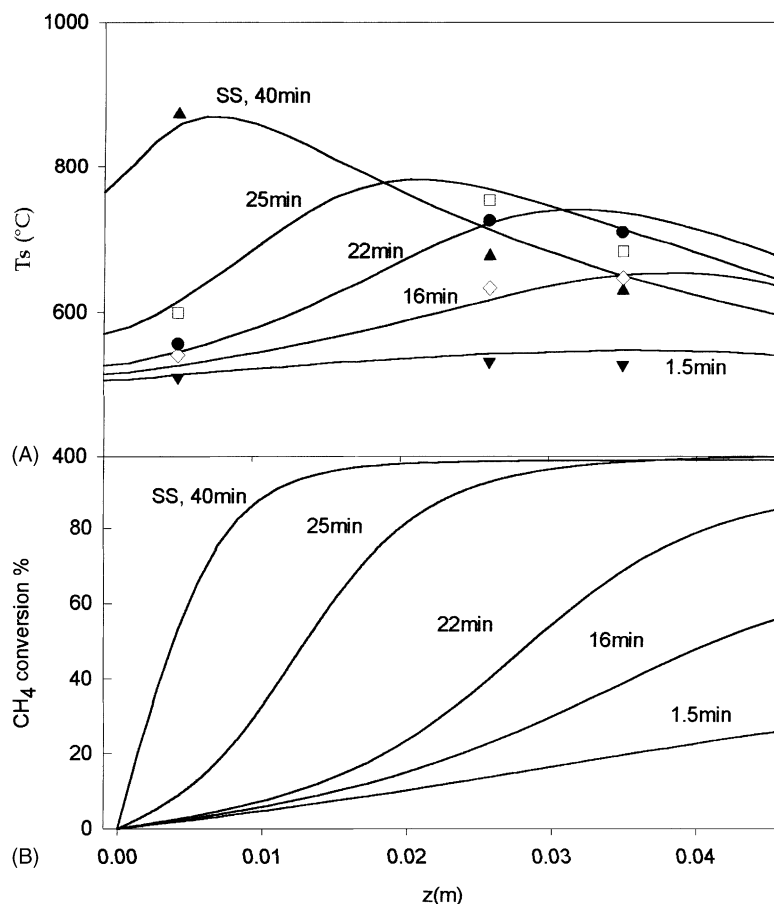


Fig. 1. Catalyst temperature (A) and CH_4 conversion (B) as functions of axial position and different run times: (\blacktriangledown) 1.5 min; (\diamond) 16 min; (\bullet) 22 min; (\square) 25 min; (\blacktriangle) steady-state (40 min). Experimental conditions: $T_{\text{preheat}} = 485^\circ\text{C}$; $\lambda_{\text{CH}_4}^{\text{in}} = 3\%$; $v_g = 1.5 \text{ m/s}$; $\lambda_s = 3 \text{ W/m K}$. Solid lines represent the values of model simulations.

external heat losses. At steady state roughly 65% of the total heat produced by combustion is lost towards the environment. Of this only 10% is radiated through the inlet and outlet sections while the remaining 90% is transferred in the radial direction by conduction through the external walls. Nevertheless, inclusion of radiation heat exchange mechanism through the external sections of the monolith is necessary to correctly model the transient behaviour as demonstrated in Fig. 2, where the solid temperature at $z = 0.5 \text{ cm}$ from the inlet of reactor is shown for three values of the emissivity. It is possible to notice that the time required by the heat wave to travel approximately doubles when the emissivity is varied from 0.6 to 0.9, all the rest being the same.

The relevance of heat losses also emerges when performing combustion experiments at different superficial gas velocity (v_g) [11]. It was experimentally observed by slowly raising the gas inlet temperature (Fig. 3) that once light-off conditions are reached, the maximum temperature measured on the catalyst significantly increases with increasing gas velocity (from 0.75 to 2.25 m/s). This phenomenon is apparently in contrast with the corresponding reduction of the contact time. In fact the more heat produced by combustion at higher gas flow rate can cause a relevant increase in catalyst temperature if non-adiabatic conditions apply. Fig. 3 shows that model simulations reproduce the same behaviour experimentally observed; moreover it reveals that if a too high value

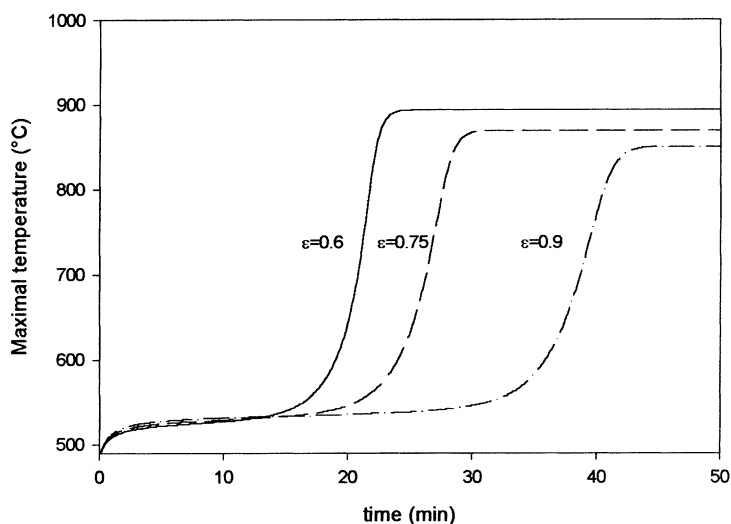


Fig. 2. Maximum catalyst temperature ($x = 0.005$ m) as a function of time for three different values of the emissivity. Simulations conditions: $T_{\text{preheat}} = 485$ °C; $x_{\text{CH}_4}^{\text{in}} = 3\%$; $v_g = 1.5$ m/s.

of the gas velocity is used (i.e. $v_g = 4.7$ m/s), the reaction does not ignite at all at the inlet gas temperatures explored so that the conversion of methane and the temperature raise result negligible.

The above described effect of gas velocity appears significantly different from the literature results for

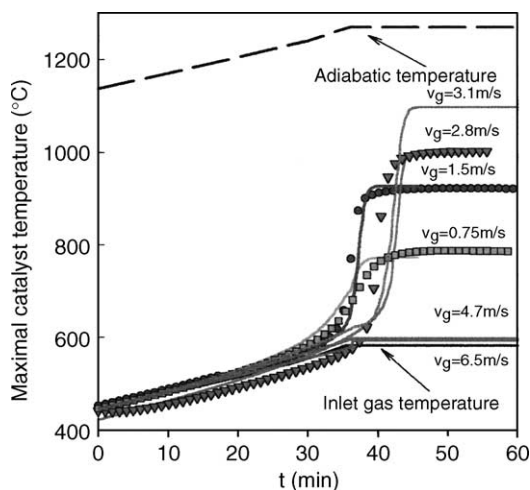


Fig. 3. Maximum catalyst temperature as a function of time at different values of gas superficial velocity. T_{preheat} varied linearly at a rate of 4 °C/min. Symbols are the experimental values, solid lines are the calculated profiles. $x_{\text{CH}_4}^{\text{in}} = 3\%$.

adiabatic reactors [1,4]. The commonly simulated behaviour for such monolithic reactors is indeed that on increasing gas flow rate, catalyst temperature decreases due to the decrease of contact time and consequently of the fuel conversion. Conversely in the presence of heat losses, an increase of superficial gas velocity corresponds to an increase of the degree of adiabaticity of the system, as long as the reaction is ignited. A similar effect of gas velocity in monolithic catalysts has been already described in other lab-scale reactors, as, for example, in short contact time reactors for partial oxidation processes, where increasing the gas flow rate, both temperature and alkane conversion increase while contact time becomes shorter [18,19].

The catalytic combustor may exhibit a steady-state multiplicity typical of highly exothermic reactions. Fig. 4 shows that at least two stable steady states exist, resulting in different values of the ignition and extinction temperatures with an hysteresis of about 55 °C [11].

Upon decreasing the gas inlet temperature from ignited conditions, the stationary temperature profile moves its maximum towards reactor exit while the overall conversion remains almost unaffected as long as the light-off point is kept inside the monolith [11]. This result suggests that the methane conversion is mainly determined by the hot spots, as shown in Fig. 1.

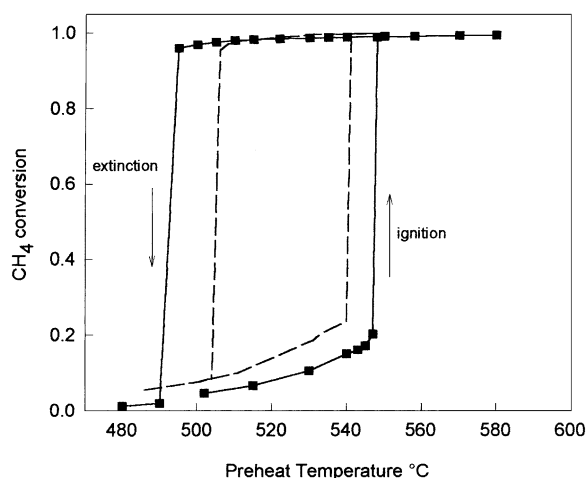


Fig. 4. Ignition–extinction cycle as obtained by simulations (---) and experiments (■) for CH_4 combustion over a 64 h aged catalyst under the following experimental conditions: $x_{\text{CH}_4}^{\text{in}} = 3\%$; $v_g = 1.5 \text{ m/s}$; $L = 0.023 \text{ m}$ [11].

The hysteresis has been simulated starting from a non-ignited condition with a uniform catalyst temperature initially equal to $T_s^0 = T_{\text{preheat}} = T_{\text{gas}}^{\text{in}}$. Subsequently, runs are performed by increasing the gas preheating ($T_{\text{gas}}^{\text{in}}$) step by step, starting from the catalyst temperature profile previously calculated at steady state. Once ignition has been obtained, the inlet gas temperature is slightly decreased starting each time from the previously calculated steady state. Fig. 4 illustrates that the model is able to reproduce qualitatively the occurrence of two stable steady-states even if the predicted hysteresis window ($\Delta T \approx 35^\circ\text{C}$) is slightly narrower. Nevertheless, since no fitting parameters have been used to reproduce the experimental behaviour, we assume this model as satisfactory in order to investigate the steady-state multiplicity.

The existence of hysteresis in monolithic reactors has been verified both experimentally [1,3,11,16] and theoretically [4,9]. Most of the experimental results are related to the catalytic oxidation of CO, mainly in automotive catalytic converter as extensively reported by Hlavacek and Votruba [16]. Hysteresis has been also observed for the catalytic oxidation of propane over noble metal catalyst [1], of methane over perovskites [11] and Pd-based [3] monoliths.

Different explanations have been proposed for the presence of the same phenomenon according to the

different processes and/or conditions adopted. In CO oxidation, it has been assumed that multiplicity occurs at the level of catalyst surface as result of a non-linear reaction rate. Hayes and Kolaczkowski [9] showed simulation results demonstrating that use of a Langmuir–Hinshelwood–Hougen–Watson reaction rate equation was essential to reproduce the hysteresis of noble metal monoliths. On the other hand, Young and Finlayson [4] numerically simulated the experimentally observed hysteresis of CO oxidation in a monolith converter, addressing the occurrence of steady-state multiplicity to the feedback induced by wall thermal conductivity. They showed that by decreasing the wall thermal conductivity the region of existence of multiple steady state (ΔT) becomes wider.

In the present model the reaction rate (5) is a power law expression which does not possess any intrinsic kinetic feedback mechanism. The simulated steady-state multiplicity then cannot be addressed to kinetics but it can be rather related to thermal mechanisms. This means that multiplicity has to be related to the interaction between heat produced by reaction and heat exchanged. At this stage it is not clear whether the thermal instability occurs at the reactor or at the catalyst level.

Hereafter, we analyse the bifurcation features of the model by taking the inlet gas temperature as bifurcation parameter and by varying the overall heat transfer coefficient (U), the gas–solid heat transfer coefficient (h_g), and the support thermal conductivity (λ_s) to get insights about the origin of the hysteresis. The bifurcation analysis carried out by means of the continuation method enables the exploration of a large space of operating parameters with dramatic savings of computational time with respect to direct simulations.

Fig. 5A–C show the bifurcation diagrams, in terms of outlet methane conversion as a function of the gas inlet temperature, obtained by varying each of the parameters in turn whilst keeping all remaining constant and set equal to the values reported in Table 1.

Each diagram is characterised by three branches representing, respectively, the locus of stable extinguished or ignited solutions (—) and unstable steady states (saddle points, ---). At low values of the inlet gas temperature, on the lower branch, only one steady state is possible, corresponding to an extinguished solution. Upon increasing the gas inlet temperature, a

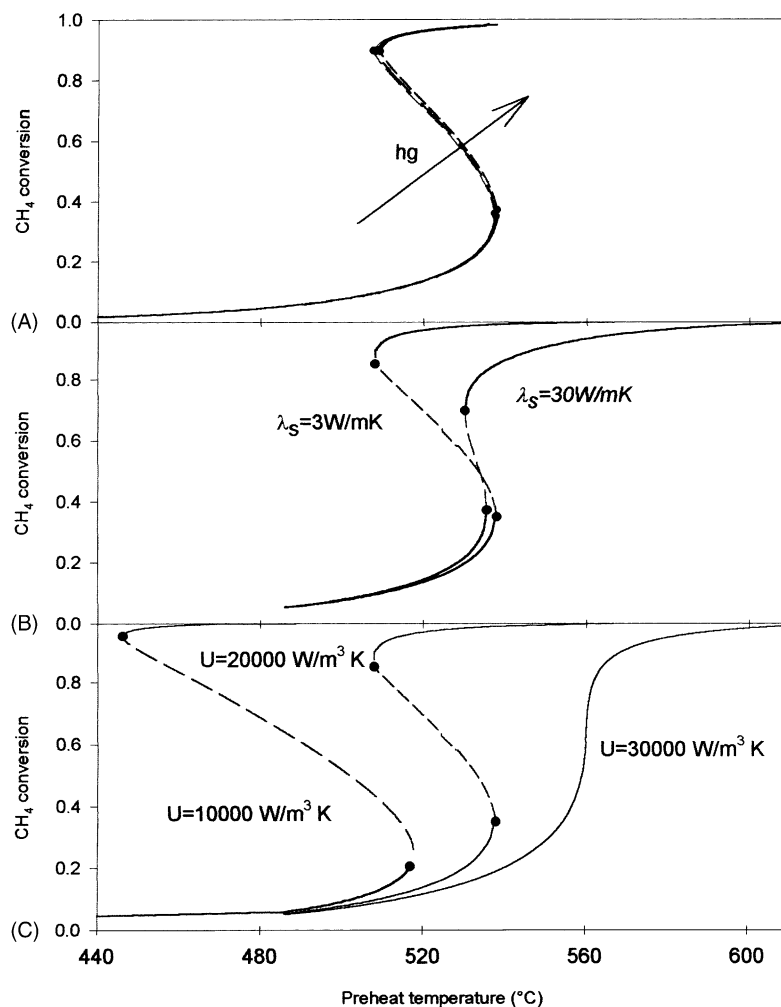


Fig. 5. Bifurcation diagrams of methane conversion as a function of preheating temperature, at different values of: (A) gas–solid heat transfer coefficient h_g 150, 210 and 300 W/m² K ($U = 20\,000\text{ W m}^{-3}\text{ K}^{-1}$, $\lambda_s = 3\text{ W m}^{-1}\text{ K}^{-1}$); (B) wall thermal conductivity λ_s ($U = 20\,000\text{ W m}^{-3}\text{ K}^{-1}$, $h_g = 210\text{ W m}^{-2}\text{ K}^{-1}$); (C) external heat transfer coefficient U ($\lambda_s = 3\text{ W m}^{-1}\text{ K}^{-1}$, $h_g = 210\text{ W m}^{-2}\text{ K}^{-1}$). Solid lines represent the locus of stable steady-states, dashed lines the locus of unstable steady-states, symbols are the limit points.

limit point (●) is reached (saddle-node bifurcation) and the solution jumps to the upper branch which is the locus of the ignited solutions. The limit point corresponds to the minimum light-off temperature. On cooling, the reactor follows the upper ignited branch until another limit point is reached (saddle-node bifurcation) where the conversion rapidly drops and extinction occurs.

Fig. 5A shows that the gas–solid heat transfer coefficient h_g has no relevant influence on the steady-state

multiplicity suggesting that multiple solutions are not related to exchange mechanisms between gas and solid phases and thus are not related to the catalyst level.

Regarding the effect of thermal conductivity (Fig. 5B) the higher the value of λ_s , the narrower is the hysteresis window. This result clearly excludes that under present conditions multiplicity of steady states is generated by the axial heat diffusion, because if this were the case a higher value of λ_s would determine a larger hysteresis. At low values of

thermal conductivity it is possible to distinguish two zones along the reactor: the first zone is dominated by reaction whilst the second one by heat exchange with the surroundings. Upon decreasing the inlet gas temperature in the ignited branch, the maximum temperature which is the separation point between these two zones moves along the channel eventually reaching the outlet and thus causing extinction. Conversely, for high values of solid thermal conductivity the reactor is almost isothermal and then the whole channel is involved in the heat losses as well as in the reaction. In this case the region of existence of multiple steady states is narrower because it is not possible anymore to distinguish between the two zones.

Finally, Fig. 5C shows that the window of the hysteresis is quite sensitive to the value of the global heat

transfer coefficient, U . It is possible to conclude that the observed hysteresis is probably generated at the reactor level, being related to the competition between the heat produced and heat lost through the external surface.

Fig. 5B shows that under non-adiabatic conditions complete fuel conversion is more difficult to achieve over metallic substrates. Indeed, comparison of conversion levels predicted by the model at same gas temperature (e.g. 560 °C) and equal values of all parameters except conductivity, shows that for $\lambda_s = 3 \text{ W/m K}$ methane conversion results significantly higher than at $\lambda_s = 30 \text{ W/m K}$ (about 99% vs. 96%). It is worth noting that we did not find any Hopf bifurcation points suggesting that according to the present model no limit cycles are possible and thus no stable oscillations can be predicted.

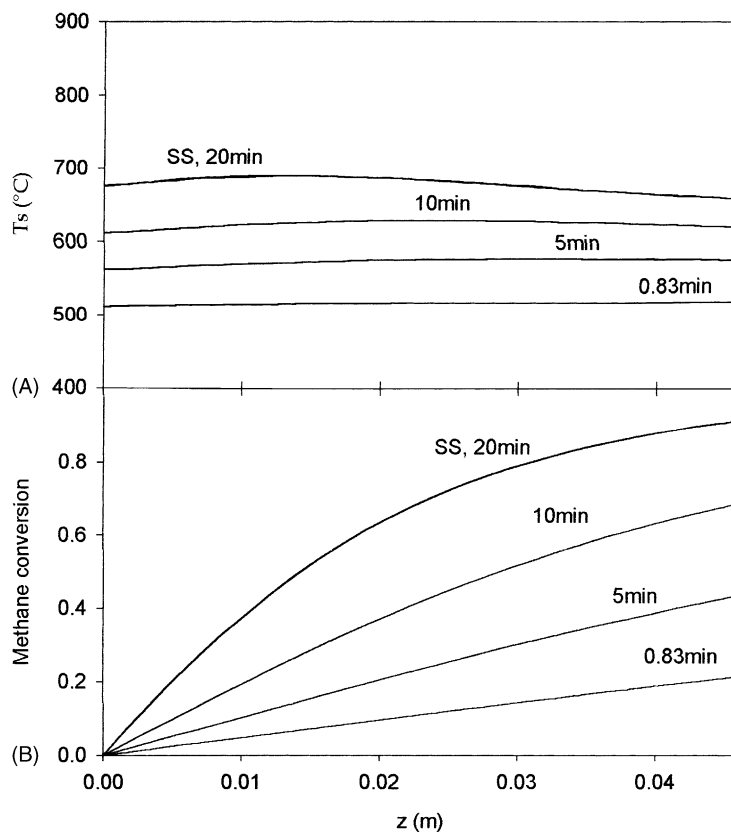


Fig. 6. Model predicted axial profiles of catalyst temperature (A) and CH_4 conversion (B) at different times during ignition. Simulation conditions: $T_{\text{preheat}} = 485^\circ\text{C}$; $x_{\text{CH}_4}^{\text{in}} = 3\%$; $v_g = 1.5 \text{ m/s}$; $\lambda_s = 30 \text{ W/m K}$.

The transient behaviour during the heating-up of the monolith is strongly influenced by the value of the axial thermal conductivity. With increasing axial thermal conductivity, the predicted axial temperature profiles become more similar to those in an isothermal reactor. At the same time, the maximum surface temperature decreases.

In contrast to that observed for the ceramic monolith (Fig. 1A), the absence of peak temperatures prevents the system from reaching complete fuel conversion (Fig. 6B), as pointed out by the bifurcation analysis. Use of metal substrates may be beneficial to both control temperature and reduce catalyst thermal stresses, not only at steady state as already pointed out by Groppi et al. [32], but also during transient phases (Fig. 6A).

In conclusion, use of ceramic substrates for developing structured catalysts for high temperature methane combustion seems recommendable for applications such as radiant burners, where the existence of hot-regions is beneficial to increase the fraction of heat transferred via radiation, while conversion is consequently very high also under non-adiabatic conditions. Conversely, low thermal conductivity supports can be dangerous for the catalyst lifetime for the appearance of hot spots. Such phenomenon may be even more dramatic under transient operations. Fig. 7 compares response of monoliths with different thermal conductivity to a step change of gas velocity from a value corresponding to an ignited solution ($v_g = 1.5$ m/s) to an extinguished value ($v_g = 6.5$ m/s).

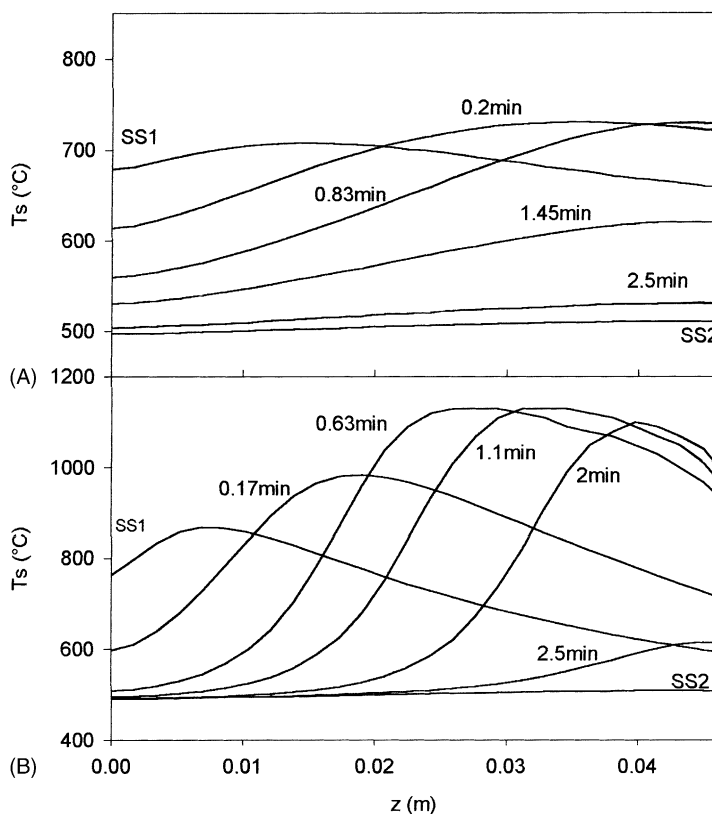


Fig. 7. Predicted axial temperature profile in the catalyst after a step change of gas velocity from $v_g = 1.5$ m/s (ignited steady state: SS1) up to $v_g = 6.5$ m/s (extinguished steady state: SS2), at two values of thermal conductivity: (A) $\lambda_s = 30 \text{ W m}^{-1} \text{ K}^{-1}$; (B) $\lambda_s = 3 \text{ W m}^{-1} \text{ K}^{-1}$. Simulation conditions: $T_{\text{preheat}} = 485^\circ \text{C}$; $x_{\text{CH}_4}^{\text{in}} = 3\%$.

For a high thermal conductivity monolith (Fig. 7A) the temperature at each axial position decreases from its value at ignited steady state (SS1) to the final extinguished value (SS2). The enhanced heat transfer in the axial direction determines a rapid cooling of the catalyst after the increase of flow rate. On the contrary, with lower λ_s , the system moves from the ignited steady-state operating point (SS1), to the extinguished operating point (SS2) experiencing transient local over-heating, as revealed by catalyst temperatures higher than in both SS1 and SS2 (Fig. 7B).

At the increased gas velocity, the reaction front is eventually blown out of the reactor, causing the system to be at the extinguished operating point (SS2). Temporary overheating of the catalyst occurs due to the difference in advective propagation speeds of concentration and temperature disturbances. Since the temperature (and the reaction rate) changes more slowly than the concentration, the methane concentration at the moving light-off point will be temporarily higher after increasing the gas velocity, thus enhancing the magnitude of the hot spot. This phenomenon is commonly referred to as ‘wrong-way behaviour’ [17,33], and has been usually shown to occur for exothermic reactions carried out in adiabatic monoliths when gas inlet temperature is suddenly decreased below the extinction limit [2].

4. Conclusions

An unsteady one-dimensional model was developed to study the transient behaviour of a monolithic reactor and investigate the effect of the most important parameters on its performance.

Hot spots are found in ceramic monolithic catalysts for both steady state and transient operations. Over such catalysts, the presence of hot regions has beneficial effects in achieving complete fuel conversion but also negative consequences on the catalyst durability.

Model simulations reveal that at higher values of thermal conductivity (metal monoliths) the catalyst does not exhibit hot spots both in time and space during start-up. Moreover, it was shown that after a step change of flow rate the wrong-way behaviour typical of ceramic supports does not occur in higher thermal conductivity monoliths due to a nearly isothermal reactor behaviour. As the support thermal conductivity

is increased thermal stresses over the catalyst surface are reduced and its lifetime increased. However, complete fuel conversion is reached at higher values of the inlet gas temperature.

The bifurcation analysis applied to the developed model allows the understanding of the nature of the steady-state multiplicity experimentally observed when the gas inlet temperature is changed. Such hysteresis is attributed to thermal effects and in particular, to the competition between heat losses and heat produced by reaction.

References

- [1] R. Prasad, H.L. Tsai, L.A. Kennedy, E. Ruckenstein, *Combust. Sci. Technol.* 26 (1981) 51.
- [2] T. Ahn, W.V. Pinczewski, D.L. Trimm, *Chem. Eng. Sci.* 41 (1986) 55.
- [3] R.A. Dalla Betta, J.C. Schlatter, D.Y. Kee, D.G. Loffler, T. Shoji, *Catal. Today* 26 (1995) 329.
- [4] L.C. Young, B.A. Finlayson, *AIChE J.* 25 (1979) 192.
- [5] L.C. Young, B.A. Finlayson, *AIChE J.* 22 (1976) 331.
- [6] L.C. Young, B.A. Finlayson, *AIChE J.* 22 (1976) 343.
- [7] S.H. Oh, J.C. Cavendish, *Ind. Eng. Chem. Prod. Res. Dev.* 21 (1982) 29.
- [8] V. Cominos, A. Gavrilidis, *Chem. Eng. Sci.* 56 (2001) 3455.
- [9] R.E. Hayes, S.T. Kolaczowski, *Introduction to Catalytic Combustion*, Gordon and Breach, Amsterdam, 1997.
- [10] R.E. Hayes, S. Kolaczowski, J. Thomas, J. Titiloye, *Ind. Eng. Chem. Res.* 35 (1996) 406.
- [11] S. Cimino, A. Di Benedetto, R. Pirone, G. Russo, *Catal. Today* 69 (2001) 95.
- [12] S. Cimino, R. Pirone, G. Russo, *Ind. Eng. Chem.* 40 (2001) 80.
- [13] J.S. T'ien, *Combust. Sci. Technol.* 26 (1981) 65.
- [14] K. Zygourakis, *Chem. Eng. Sci.* 44 (1989) 2075.
- [15] R.E. Hayes, S.T. Kolaczowski, *Chem. Eng. Sci.* 49 (1994) 3587.
- [16] V. Hlavacek, J. Votruba, *Adv. Catal.* 27 (1978) 59.
- [17] K.R. Westerterp, W.P.M. van Swaij, A.A.C.M. Beenackers, *Chemical Reactor Design and Operation*, Wiley, New York, 1990.
- [18] M. Huff, L.D. Schmidt, *J. Phys. Chem.* 97 (1993) 11815.
- [19] F. Donsi, R. Pirone, G. Russo, *J. Catal.* 209 (2002) 51.
- [20] N. Gupta, V. Balakotaiah, D.H. West, *Chem. Eng. Sci.* 56 (2001) 1435.
- [21] R.D. Hawthorn, *AIChE Symp. Ser.* 70 (1974) 428.
- [22] U. Ullah, S.P. Waldrum, C.J. Bennett, T. Truex, *Chem. Eng. Sci.* 47 (1992) 2413.
- [23] J. Votruba, J. Sinkule, V. Hlavacek, J. Skrivanek, *Chem. Eng. Sci.* 30 (1975) 117.
- [24] R.E. Hayes, S.T. Kolaczowski, *Catal. Today* 47 (1999) 295.
- [25] G. Groppi, A. Belloli, E. Tronconi, P. Forzatti, *Chem. Eng. Sci.* 50 (1995) 2705.

- [26] G. Groppi, E. Tronconi, *AIChE J.* 42 (1996) 2382.
- [27] C.W. Gear, *Numerical Value Problems in Ordinary Differential Equations*, Prentice-Hall, New Jersey, 1971.
- [28] J. Doedel, A.R. Champneys, T.F. Fairgrieve, Y.A. Kuznestov, B. Sanstede, X. Wang, *AUTO97 Continuation and Bifurcation Software for Ordinary Differential Equations*, 1997.
- [29] Maple software. <http://www.bham.ac.uk/is/site-software/Maple.htm>.
- [30] A.L. Boehman, *AIChE J.* 44 (1998) 2745.
- [31] S.-T. Lee, R. Aris, *Chem. Eng. Sci.* 32 (1977) 827.
- [32] G. Groppi, E. Tronconi, *Chem. Eng. Sci.* 55 (2000) 2161.
- [33] D. Luss, *Ind. Eng. Chem. Res.* 36 (1997) 2931.